

UNCLASSIFIED

Defense Technical Information Center
Compilation Part Notice

ADP018962

TITLE: Recent Advances in High Cycle Fatigue

DISTRIBUTION: Approved for public release, distribution unlimited

This paper is part of the following report:

TITLE: International Conference on the Mechanical Behavior of Materials
[9th], ICM-9, Held in Geneva, Switzerland on 25-29 May 2003

To order the complete compilation report, use: ADA433037

The component part is provided here to allow users access to individually authored sections of proceedings, annals, symposia, etc. However, the component should be considered within the context of the overall compilation report and not as a stand-alone technical report.

The following component part numbers comprise the compilation report:

ADP018903 thru ADP019136

UNCLASSIFIED

RECENT ADVANCES IN HIGH CYCLE FATIGUE*

Ted Nicholas

Air Force Institute of Technology (AFIT/ENY)

Wright-Patterson AFB, OH 45433, USA

theodore.nicholas@afit.edu

ABSTRACT

High cycle fatigue (HCF) has been the cause of a number of turbine engine failures over the last several years within the U.S. Air Force. Extensive investigations have determined that the root cause, when related to material properties, is the accumulation of damage prior to and during service which, in turn, reduces the capability of the material in terms of the fatigue limit strength. Numerous studies have been conducted over the past several years to address the determination of fatigue limits. In this paper, in addition to developing approaches for predicting fatigue limits under various mean stresses and biaxial stress states, methods are presented for accounting for service-induced damage. One of the types of damage involves low cycle fatigue (LCF) which, by itself, should not cause failure but may reduce the HCF capability of the material. Data on the accumulation of damage under LCF or HCF overload transients, and their effects on the HCF strength of a titanium alloy are used to illustrate the inability of linear damage summation laws. A Kitagawa diagram with a short crack correction is found to be useful in assessing the fatigue strength of both smooth and notched specimens.

INTRODUCTION

Damage tolerance in structural design involves the assumption of initial or service induced damage, usually in the form of cracks, and inspection procedures to insure that any crack below the inspection limit will not grow to a catastrophic size before either the next inspection, or for the life of the part. While this approach has been highly successful in avoiding low cycle fatigue (LCF) failures in U.S. Air Force gas turbine engines since the inception of damage tolerance and retirement-for-cause policies in the 1980's, a similar approach cannot be used for high cycle fatigue (HCF) design. The very high frequencies and large numbers of cycles that can be accumulated under HCF in a very short time period, combined with the very large fraction of life consumed in crack nucleation, make it impractical to inspect for cracks and apply damage tolerance principles. Rather, the approach to HCF has to be based on threshold or endurance limit concepts that involve determining stress levels below which failures due to HCF will not occur. Such an approach to pristine materials requires an extensive database, simple models for interpolating among mean stresses, and modeling concepts for biaxial stress conditions. Issues such as phase angles in biaxial loading, frequency effects, load sequencing, and others start to make such predictions much more difficult. Another aspect that must be addressed is the degradation of the fatigue strength with time in service due to damage accumulation. Such damage may be instantaneous, such as from foreign object damage (FOD), or gradually accumulated such as from fretting fatigue or LCF where cracks might form and continue to grow due to repeated loading during service. In fact, FOD, fretting fatigue, and LCF have been identified as the

* The views expressed in this article are those of the author and do not reflect the official policy or position of the United States Air Force, Department of Defense, or the US Government.

three primary concerns in the U.S. Air Force HCF program for addressing the tolerance of materials to HCF subjected to in-service damage. The subjects of FOD and fretting fatigue are touched upon in other papers in this conference [1,2], so this paper will concentrate only on some issues with respect to fatigue limit stresses in both smooth bars and specimens subjected to prior loading histories and associated damage in the form of LCF loading.

TOTAL LIFE APPROACHES

The terminology total life refers to determination of the fatigue limit strength for HCF at cycle counts that exceed the possible exposure of a material during service without consideration of nucleation or crack propagation as individual events. It is well known that in the HCF regime, nucleation comprises a large majority of a materials life. As an example, Morrissey et al. [3] have calculated crack growth lives for titanium cylindrical specimens and show that at a total life of 10^7 cycles, approximately 98% of life is consumed in nucleating a crack to a length of 57 μm .

To represent the stress corresponding to a total life of, say 10^7 cycles, a plot can be made of these stresses as a function of stress ratio (R = ratio of minimum to maximum stress). Alternately, data can be plotted as a function of mean stress. The Haigh diagram, incorrectly referred to as a Goodman diagram, is a common method of representing the fatigue limit or endurance limit stress of a material in terms of alternating stress, defined as half of the vibratory stress amplitude. Thus, the maximum dynamic stress is the sum of the mean and alternating stresses. For many rotating components, the mean stress is known fairly accurately from the rotational speed, but the alternating stress is less well defined because it depends on the vibratory characteristics of the component. Thus a Haigh diagram represents the allowable vibratory stress as the vertical axis as a function of mean or steady stress on the x-axis. Many attempts have been made to define the equation which best represents the data on a Haigh diagram [4]. Goodman [5] proposed use of the “dynamic theory” which results in a straight line when the allowable alternating stress is taken equal to half the ultimate stress. Of interest is that Goodman proposed such an equation as one that is “very easy of application and is, moreover, simple to remember” [5]. He also noted that “whether the assumptions of the theory are justifiable or not is quite an open question.”

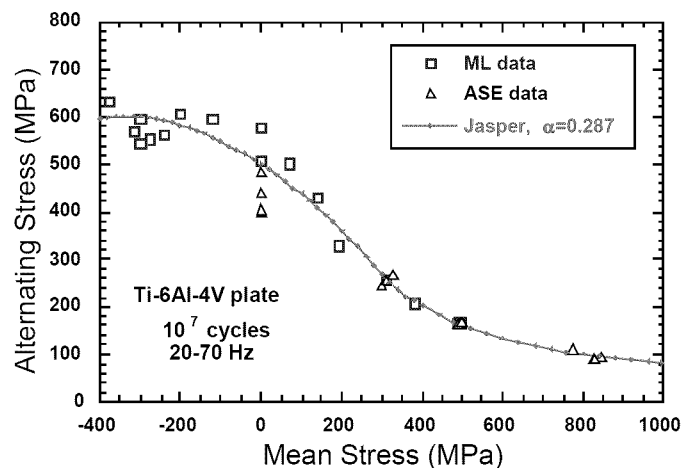


Figure 1. Haigh diagram for Ti-6Al-4V plate with modified Jasper equation fit [4].

Recent work by Nicholas and Maxwell [4] has shown that a modified version of the constant energy density range theory of Jasper [6] can represent fatigue strength at 10^7 cycles in a Ti-6Al-4V titanium alloy over a wide range of stress ratios (or mean stresses) including data in the negative mean stress region. Figure 1 shows the fit to the data, which involves use of an empirical constant in the theory to account for the observation that compressive stresses contribute less than tensile stresses in fatigue.

The Jasper approach, described in detail in [4], computes the stored energy density range per cycle. For uniaxial loading, assuming purely elastic behavior (a reasonable assumption for HCF), where stress and strain are related by $\sigma = E\varepsilon$, the stored energy density range is

$$U = \frac{1}{2E} \left(\sigma_{\max}^2 \pm \sigma_{\min}^2 \right) \quad (1)$$

where E is Young's modulus, the plus sign is for stress ratio $R < 0$ and the minus sign for stress ratio $R > 0$. For the specific case of fully reversed loading, where $R = -1$, the energy is

$$U = \frac{1}{2E} \left(2 \sigma_{-1}^2 \right) \quad (2)$$

where σ_{-1} represents the alternating stress (= maximum stress) at $R = -1$. For any other case of uniaxial loading, the following equation is easily derived and can be used to obtain the value of the alternating stress on a Haigh diagram:

$$\sigma_a = \frac{\sigma_{-1}}{\sqrt{2}} \sqrt{\frac{(1-R)^2}{1-R|R|}} \quad (3)$$

For fatigue involving cycling into compression, it is postulated that stored energy density per cycle does not contribute towards the fatigue process as much when the stresses are compressive as when they are in tension. Assuming that compressive stress energy contributes a fraction, α , compared to comparable energy in tension, then the total effective energy is formulated in the following manner, where $0 < \alpha < 1$:

$$U_{\text{tot}} = U_{\text{tens}} + \alpha U_{\text{comp}} = \text{constant} \quad (4)$$

In the use of this equation, energy terms corresponding to negative stresses have to be modified by the coefficient α . The introduction of the constant α has the effect of modifying the shape of the Jasper equation to fit data at negative mean stresses as illustrated in Fig. 1, where $\alpha = 0.287$ was obtained by fitting Eq. (4) to experimental data obtained at $-4 < R < 0.8$ and particularly at values of stress ratio $R < -1$ corresponding to negative mean stresses.

The extension of the modified Jasper equation to biaxial loading is not straightforward because compression energy is calculated differently than tension energy for the same stress range. For the case of pure torsion, the stress state due to shear of magnitude τ_0 is equivalent to tension and compression on orthogonal planes of magnitude τ_0 and $-\tau_0$, respectively, oriented 45 degrees to the shear case. It is not obvious how to calculate fatigue energy in torsion since it is not an invariant, given the postulated difference between tension and compression energy. As an engineering solution, it is proposed that energy be calculated based on stresses in the principal directions, where shear stresses are zero. The calculations

for this case are then straightforward, where the relations between stress and strain make use of the two-dimensional equations of elasticity in plane stress. The results are presented in Fig. 2 which shows the computed fatigue endurance limit under pure tension, σ_{tens} , divided by the computed fatigue (endurance) limit in the x direction, $\sigma_{x,\text{end}}$ as a function of the ratio of the applied stress in the y direction, $\sigma_{y,\text{app}}$, divided by the applied stress in the x direction, $\sigma_{x,\text{app}}$. For comparison, the same quantities are computed for a von Mises equivalent stress.

Two data points are shown in Fig. 2 for fatigue limit stresses in torsion corresponding to a life of 10^6 cycles. The results were obtained on rectangular cross-section specimens of dimensions 17.3 mm x 3.18 mm tested at 10 Hz. These specimens were tested as part of an ongoing FOD study. The reference stresses for the uniaxial case are based on data from other studies [7] and use of the modified Jasper Eq. (3) to fit the data and extrapolate to different values of R. It can be seen that the principle stress energy formulation using the compression energy modification provides a reasonable correlation of the torsion fatigue data.

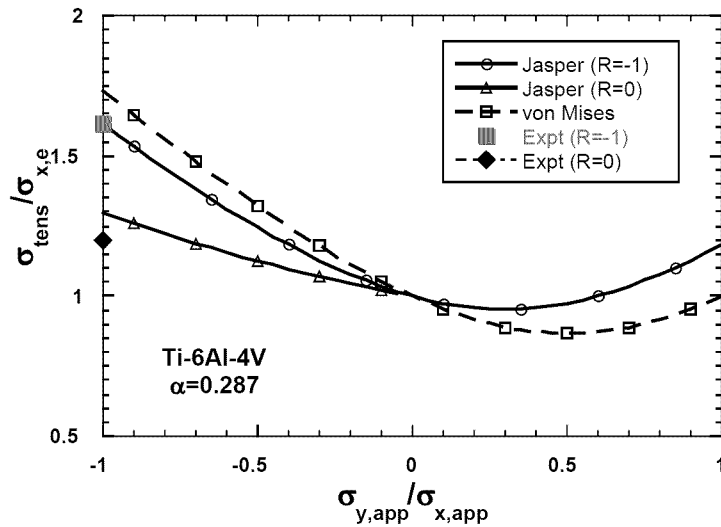


Figure 2. Predictions of fatigue limit stress as a function of applied biaxial stress state.

LCF/HCF INTERACTIONS

Several series of tests have been conducted over the years in our laboratory at AFRL/ML where specimens have been subjected to LCF loading prior to HCF testing to obtain a fatigue limit stress. In these types of tests, the LCF stress corresponding to a life in the typical range 10^4 to 10^5 cycles is determined first from a series of LCF tests and then interpolating on a S-N curve. Some fraction of the LCF life is then applied to the specimen after which it is tested in HCF using the step-loading technique [8] where load-history effects and coxing have been shown not to be important in Ti-6Al-4V [9]. Two things should be noted in this type of experiment involving preloading under LCF. First, the LCF life is a statistical variable, so testing up to a predetermined fraction of predicted life has an inherent error associated with what fraction of life it really was. Second, if LCF testing and HCF testing are performed at the same value of stress ratio, R, then the LCF test will be at a larger stress than the HCF test for

an uncracked specimen. In the event that a crack is formed during LCF, application of a lower load during HCF testing can amount to an overload effect, so the fatigue limit may tend to be higher than that obtained without an overload effect. Such a phenomenon was demonstrated by Moshier et al [10] and is discussed below.

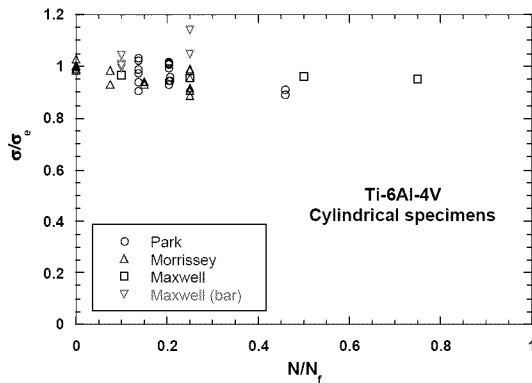


Figure 3. Normalized endurance limit stress as function of LCF history.

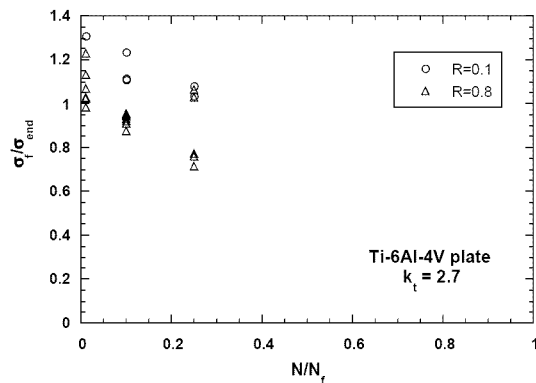


Figure 4. Fatigue strength of notched specimens subjected to prior LCF [7].

Data obtained from different tests on smooth bars subjected to LCF, then HCF, are summarized in Fig. 3, where the fatigue limit stress is normalized against the data for tests without any prior history. The horizontal axis is the number of LCF cycles divided by the expected life at the stress level and R used in the LCF tests. Noting that from a design perspective that the allowable LCF life would be much less than the average, LCF cycle ratios in practice should not be expected to exceed 0.5 of the average, and even less when factors of safety are included. Thus, any reasonable number of LCF cycles that might be encountered are expected to be confined only to the left portion of Fig. 3. The data show, that within reasonable scatter, the HCF limit does not appear to be degraded by any significant amount in tests covering a range of LCF stress levels and corresponding lives, and stress ratios in both LCF and HCF. Data designated Park and Morrissey appear in [11] and [3], respectively.

Similar data obtained from tests on notched specimens are presented in Fig. 4. In these cases, preloading in LCF often involved testing at stress levels that produced plastic deformation near the notch root. The plastic strain field was normally larger than that obtained under pure HCF with no preload, so the comparison of data from LCF/HCF tests with pure HCF tests is much more complicated than in the smooth bar case. In the case of specimens tested at $R=0.8$, the high peak stresses under HCF combined with the plastic deformation occurring under the prior LCF makes the comparisons even more difficult. It should be noted that in at least two cases of this type of LCF/HCF loading, a crack was found on the fracture surface which indicated that the LCF produced initial cracking which resulted in a reduction of subsequent HCF strength [7]. The effect of precracking is discussed below. Nonetheless, the reduction of fatigue strength due to LCF in notched specimens does not appear to be very significant until at least 25% of LCF life has been expended. As pointed out above, this is based on average life so that with scatter and a factor of safety, it is not reasonable to expect that a material would be subjected to 25% of *average* life in service.

To further study the possibility of cracks forming under LCF, tests were conducted on specimens subjected to prior HCF at a value of $R=-3.5$ at a stress level of 240 MPa, which is below the observed failure stress of 265 MPa at that value of R . It is postulated that cracks nucleate due to some function of total stress or strain range, but will only continue to propagate when subjected to a positive stress range that produces a positive crack driving force, K . After subjecting the specimens to 10^7 cycles at $R=-3.5$, the specimens were then tested in HCF until failure at either $R=0.1$ or $R=0.5$ using the step-loading procedure. Some of the specimens were stress relieved after the initial loading at $R=-3.5$ in order to remove any history effects on a crack that may have formed. The results are summarized in Fig. 5 where baseline tests are compared with preload tests with and without stress relief (SR) for both values of R . Note that the peak stress levels applied in the HCF tests are considerably higher than the peak stress used in the preloading (240 MPa). Expanding the stress scale indicates that a minor reduction in HCF strength may have been obtained due to preloading at $R=-3.5$, but the magnitude of any such reduction is not very significant.

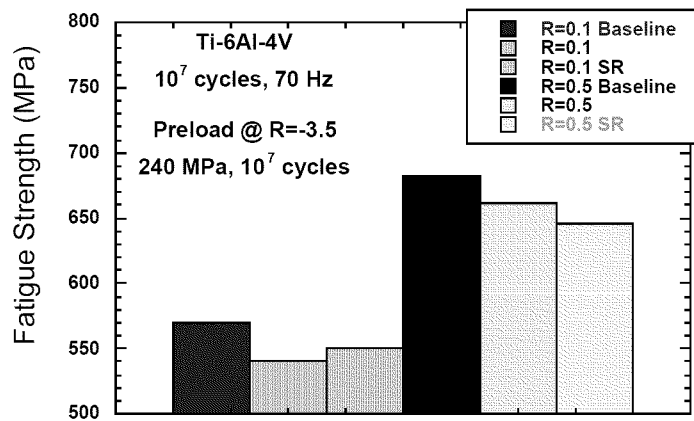


Figure 5. Fatigue limit stress for specimens subjected to preloads at $R=-3.5$.

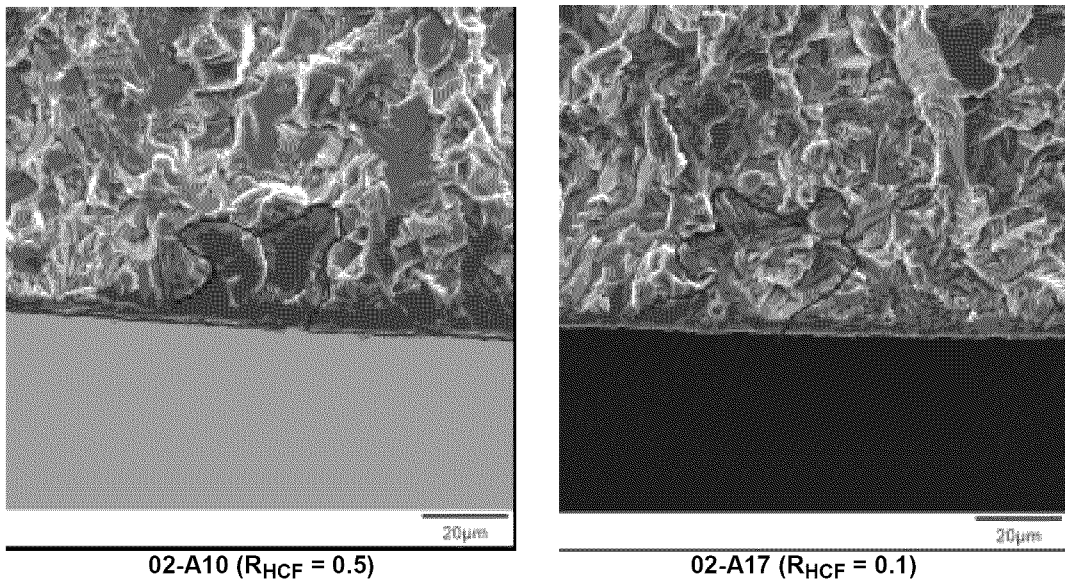


Figure 6. Fracture surfaces of specimens subjected to preload at $R=-3.5$.

Following the reasoning above, where nucleation might be expected at stress levels below those for propagation when R is negative, the fracture surfaces of several of the specimens pretested at R=-3.5 and then failed at positive values of R were observed under SEM and are shown in Fig. 6. While the observations on these two specimens which had somewhat lower fatigue limit stresses are not entirely conclusive, there are indications, as outlined in the pictures, that a crack might have formed during the R=-3.5 testing. Such features were not observed in baseline specimens which received no stressing at negative R. Of significance is the size of the possible cracks seen which appear to be no deeper than 30 or 40 μm .

FRACTURE MECHANICS APPROACHES

The reduction of the HCF capability of a material due to a crack can be evaluated with the aid of a Kitagawa type diagram [12] shown schematically in Fig. 7. This plot of stress against crack length on log-log scales was first suggested for a simple edge crack geometry where stress intensity is proportional to $a^{-0.5}$. The endurance limit when no crack is present, or the threshold stress intensity when there is a crack, represent the limits above which failure will occur and below which it will not, corresponding to some chosen number of cycles or crack growth rate, respectively. The endurance limit is a horizontal line in Fig. 7 while the threshold stress intensity is line of slope = -0.5 for the simple single edge crack. The two lines can be connected to form a single smooth curve for all crack lengths using the short crack correction proposed by El Haddad et al.[13]. The crack length corresponding to the intersection of the long crack threshold and the endurance limit is defined as a_0 in the correction. The short crack correction of El Haddad, shown graphically in Fig. 7, uses the concept that a crack of length "a" behaves as if it had a length " $a + a_0$ ", which has the long crack threshold value. It is easily shown that the fatigue limit stress for any true crack length "a" in a cracked body whose K solution for the cracked body is written as $K = \sigma \sqrt{\pi a} Y(a)$ is

$$\sigma = \frac{K_{th,LC}}{\sqrt{\pi(a + a_0)} Y(a + a_0)} \quad (5)$$

where $K_{th,LC}$ is the long crack threshold. As the crack length goes to zero, the fatigue limit stress goes to σ_e .

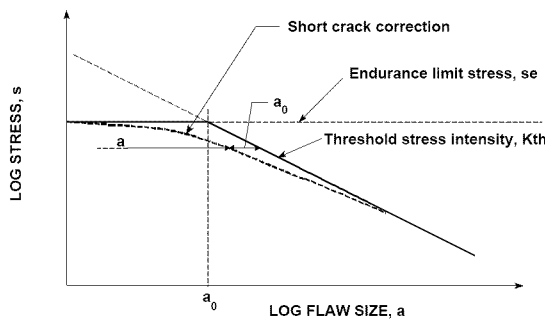


Figure 7. Schematic of Kitagawa diagram.

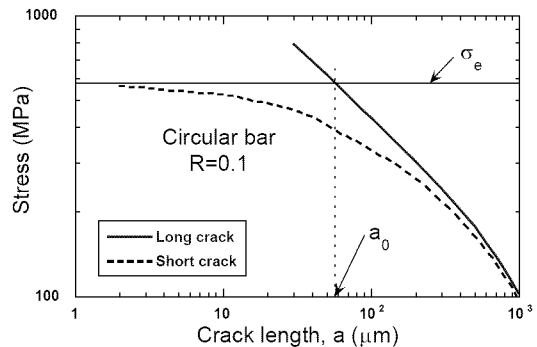


Figure 8. Kitagawa diagram for 3.8 mm diam. circular bar.

A Kitagawa diagram for a circular bar of diam. = 3.8 mm is shown in Fig. 8. Note that the long crack threshold is not a straight line but, rather, takes the form of the actual K solution for that geometry [12]. In an investigation of history effects where specimens were first subjected to stresses up to 40% above the HCF fatigue limit, no cracks were detected on the fracture surfaces [12]. However, since the detection limit is less than a_0 in this case, Fig. 8, cracks having lengths below $a_0 = 57 \mu\text{m}$ should not have a detrimental effect on fatigue limit stress. In general, the Kitagawa diagram with the short crack correction shows that if the threshold data follow the curve, that cracks of length a_0 or less have fatigue limit stresses which are not significantly lower than the endurance limit for any geometry. At a crack length of a_0 , the fatigue limit stress is $1/\sqrt{2}$ or 0.71 of the endurance limit. Thus, it is not surprising to find that small cracks formed under fretting fatigue [14,15], under LCF at notches [7,10] or in smooth bars [3,11] do not have a significant detrimental effect on the fatigue limit stress as illustrated partially in Figs. 3 and 4. The data of Fig. 5 and possible crack sizes shown in Fig. 6 also support this conclusion.

One of the more revealing studies of the application of fracture mechanics to prediction of HCF thresholds or fatigue limit stresses is the recently published work of Moshier et al. [10]. There, notched specimens were precracked in LCF and subsequently retested in HCF to determine the fatigue limit stress. Fracture mechanics was used to relate the observed stresses to stress intensities including corrections for small crack behavior using the approach suggested by El Haddad. Specimens having a notch with $k_t = 2.25$ were subjected to LCF at either $R=-1$ or $R=0.1$ until a crack was detected using an infrared detection system. Surface flaws at the notch root having depths under $20 \mu\text{m}$ were detected and subsequently heat tinted in order to be able to detect them on the subsequent fracture surface. All of the cracked specimens were then tested under HCF in order to establish the fatigue limit stress using step loading. K analysis of the surface flaw at a notch root, combined with a small crack correction, were plotted on a Kitagawa type diagram as shown in Fig. 9. Of significance is the use of a Kitagawa type diagram for geometries having cracks other than a single edge crack. In this case, the geometry is that of a double notched tension specimen. The use of the Kitagawa diagram for this geometry shows that the endurance limit and the value of a_0 for the short crack correction are not material constants but, rather, material parameters for the particular geometry and stress ratio, R , being investigated.

The maximum stress levels for LCF precracking at $R=-1$ and $R=0.1$ in Fig. 9 were below and above the stress levels that caused failure in HCF, respectively. In the formation of a crack under LCF and the subsequent propagation under HCF, these conditions would be referred to as an underload (negative overload) and overload, respectively. For the overload condition, a simple model was developed in [10] which modified the threshold K. The modified K along with the small crack correction is plotted as the thin line in Fig. 9 while the experimental data in the form of fatigue limit stress with LCF at $R=0.1$ are plotted as hollow circles. The model provides a very good representation of the data. Similarly, the data representing LCF precracking at $R=-1$ are well represented by an uncorrected threshold K with a small crack correction. The data are represented by the hollow triangles while the threshold K is shown as the thin dashed line. In this case, no underload model is needed to correct for the effective threshold. Of particular interest are the data points from precracking at either value of R where stress relief annealing was performed after the LCF precracking, denoted by SRA in

the figure. These data show that the SRA process removes any history effects and the resulting precracks follow the prediction of the long crack threshold with the a_0 short crack correction. The need for the short crack correction is easily seen by the two curves with heavy lines which represent the threshold for a long crack (dashed) and the overload corrected threshold (solid). The intersection of these curves with the endurance limit line represents the value of a_0 , the El Haddad small crack correction factor, for this geometry..

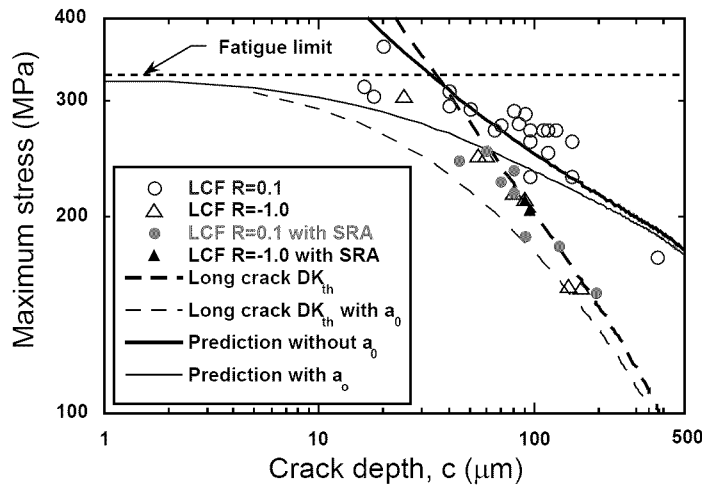


Figure 9. Experimental data and model predictions for notched specimens on a Kitagawa diagram [10].

Cracks formed under fretting fatigue have been measured after HCF testing to determine the fatigue limit stress. In two separate investigations [14,15], the crack sizes and corresponding stresses were plotted on a Kitagawa type diagram for the specific crack specimen geometry, including a small crack correction. In both cases, the data follow the curve connecting the endurance limit stress with the threshold stress intensity as shown schematically in Fig. 7, using a small crack correction. The cracks formed under fretting fatigue are subjected to a nominal stress condition of fully reversed loading, and no apparent history effect appears to be present in the two studies cited.

CONCLUSIONS

Fatigue limit stresses in smooth bars and threshold stress intensities in precracked specimens are easily accounted for by using a compression modified version of the energy based concept of Jasper, and the Kitagawa diagram with the El Haddad small crack correction, respectively. The Jasper formulation appears to be extendable to biaxial loading by considering stresses in principle directions. The Kitagawa/El Haddad approach seems able to explain the relatively small reduction in fatigue limit stress due to small cracks of the order of a_0 in length.

ACKNOWLEDGEMENTS

Much of the work described herein was conducted as part of the USAF HCF Program. The author would like to thank his many colleagues who contributed to this effort, in particular,

David Maxwell for the work on negative R effects, Ken Goecke for the torsion study, and John Porter, all of UDRI, for the excellent support in fractography throughout the program.

REFERENCES

- [1] S.R. Thompson, J.J. Ruschau and T. Nicholas, "An Assessment of Laboratory Techniques for Simulating Foreign Object Damage on a Leading Edge Geometry," (this volume).
- [2] S. Mall, "Fretting Fatigue Crack Nucleation Criterion for Ti-6Al-4V," (this volume).
- [3] R.J. Morrissey, P. Golden and T. Nicholas, "Damage Accumulation under Intermediate Cycle Fatigue," *Int. J. Fatigue* (in press).
- [4] T. Nicholas and D.C. Maxwell, *Fatigue and Fracture Mechanics: 33rd Volume, ASTM STP 1417*, W.G. Reuter and R.S. Piascik, Eds., ASTM, West Conshohocken, PA, pp. 476-492, 2002.
- [5] J. Goodman, *Mechanics Applied to Engineering*, Volume 1, 9th ed., Longmans, Green & Co., Inc., New York, p.634, 1930; see also 1st edition, p. 455, 1899.
- [6] T.M. Jasper, *Philosophical Magazine*, Series. 6, vol. 46, pp. 609-627, Oct. 1923.
- [7] D. Lanning, G.K. Haritos, T. Nicholas and D.C. Maxwell, *Fatigue Fract. Engng. Mater. Struct.*, vol. 24, pp. 565-578, 2001.
- [8] D.C. Maxwell and T. Nicholas, *Fatigue and Fracture Mechanics: 29th Volume, ASTM STP 1321*, T. L. Panontin and S. D. Sheppard, Eds., ASTM, West Conshohocken, PA, pp. 626-641, 1999.
- [9] T. Nicholas, *Fatigue Fract. Engng. Mater. Struct.*, vol. 25, pp. 861-869, 2002.
- [10] M.A. Moshier, T. Nicholas and B.M. Hillberry, *Fatigue and Fracture Mechanics: 33rd Volume, ASTM STP 1417*, W.G. Reuter and R.S. Piascik, Eds., ASTM, West Conshohocken, PA, pp. 129-146, 2002.
- [11] S. Mall, T. Nicholas and T.-W. Park, "Effect of Pre-Damage from Low Cycle Fatigue on High Cycle Fatigue Strength of Ti-6Al-4V," *Int. J. Fatigue* (in press).
- [12] H. Kitagawa and S. Takahashi, *Proc. of Second International Conference on Mechanical Behaviour of Materials*, Boston, MA, pp. 627-631, 1976.
- [13] M.H. El Haddad, K.N. Smith, and T.H Topper, *Journal of Engineering Materials and Technology*, vol. 101, pp. 42-46. 1979.
- [14] A.L Hutson, C. Neslen and T. Nicholas, *Tribology International*, vol. 36, pp 133-143, 2003.
- [15] P.J. Golden, B.B. Bartha, A.F. Grandt, Jr. and T. Nicholas, "Measurement of the Fatigue Crack Propagation Threshold of Fretting Cracks in Ti-6Al-4V," *Int. J. Fatigue* (in press).